Regge and GPD Comparison of Beam Spin Asymmetry in Exclusive Pion Electroproduction

A.C. Postuma,[1] G.M. Huber,[1] T.K. Choi,[2] D. Gaskell,[3] N. Heinrich,[1] T. Horn,[4,3] M. Junaid,[1] S.J.D. Kay,[1,5] K.-J. Kong,[6] V. Kumar,[1] P. Markowitz,[7] J. Roche,[8] R. Trotta,[4] A. Usman,[1] B.-G. Yu,[6] S. Ali,[4] R. Ambrose,[1] D. Androic,[9] W. Armstrong,[10,11] A. Bandari,[12] V. Berdnikov,[4] H. Bhatt,[13] D. Bhetuwal,[13] D. Biswas,[14,15] M. Boer,[10,15] P. Bosted,[12] E. Brash,[16] A. Camsonne,[3] J.P. Chen,[3] J. Chen,[12] M. Chen,[17] M.E. Christy,[14] S. Covrig,[3] W. Deconinck,[12,18] M. Diefenthaler,[3] B. Duran,[10] D. Dutta,[13] M. Elaasar,[19] R. Ent,[3] H. Fenker,[3] E. Fuchey,[20] D. Hamilton,[21] J.O. Hansen,[3] F. Hauenstein,[22] S. Jia,[10] M.K. Jones,[3] S. Joosten,[11] M.L. Kabir,[13] A. Karki,[13] C. Keppel,[3] E. Kinney,[23] N. Lashley-Colthirst,[14] W.B. Li,[12,24] D. Mack,[3] S. Malace,[3] M. McCaughan,[3] Z.E. Meziani,[10,11] R. Michaels,[3] R. Montgomery,[21] M. Muhoza,[4] C. Munoz Camacho,[25] G. Niculescu,[26] I. Niculescu,[26] Z. Papandreou,[1] S. Park,[24] E. Pooser,[3] M. Rehfuss,[10] B. Sawatzky,[3] G.R. Smith,[3] H. Szumila-Vance,[3] A. Teymurazyan,[1] H. Voskanyan,[27] B. Wojtsekhowski,[3] S.A. Wood,[3] C. Yero,[7] J. Zhang,[17] and X. Zheng[17]

(KaonLT Collaboration)

[1] *University of Regina, Regina, Saskatchewan S4S 0A2, Canada*
[2] *Department of Physics, Yonsei University, Wonju 26493, Korea*
[3] *Thomas Jefferson National Accelerator Facility, Newport News, Virginia 23606, USA*
[4] *Catholic University of America, Washington, DC 20064, USA*
[5] *University of York, York YO10 5DD, United Kingdom*
[6] *Research Institute of Basic Sciences, Korea Aerospace University, Goyang 10540, Korea*
[7] *Florida International University, University Park, Florida 33199, USA*
[8] *Ohio University, Athens, Ohio 45701, USA*
[9] *University of Zagreb, Zagreb 10000, Croatia*
[10] *Temple University, Philadelphia, Pennsylvania 19122, USA*
[11] *Argonne National Laboratory, Lemont, Illinois 60439, USA*
[12] *College of William & Mary, Williamsburg, Virginia 23185, USA*
[13] *Mississippi State University, Mississippi State, Mississippi 39762, USA*
[14] *Hampton University, Hampton, Virginia 23669, USA*
[15] *Virginia Tech, Blacksburg, Virginia 24061, USA*
[16] *Christopher Newport University, Newport News, Virginia 23606, USA*
[17] *University of Virginia, Charlottesville, Virginia 22903, USA*
[18] *University of Manitoba, Winnipeg, Manitoba R3T 2N2, Canada*
[19] *Southern University at New Orleans, New Orleans, Louisiana 70126,USA*
[20] *University of Connecticut, Storrs, Connecticut 06269, USA*
[21] *University of Glasgow, Glasgow G12 8QQ, United Kingdom*
[22] *Old Dominion University, Norfolk, Virginia 23529, USA*
[23] *University of Colorado, Boulder, Colorado 80309, USA*
[24] *Stony Brook University, Stony Brook, New York 11794, USA*
[25] *Institut de Physique Nucléaire, Orsay F-91406, France*
[26] *James Madison University, Harrisonburg, Virginia 22807, USA*
[27] *A.I. Alikhanyan National Science Laboratory (Yerevan Physics Institute), Yerevan 0036, Armenia*

(Dated: June 27, 2024)

The cross section ratio $\sigma_{LT'}/\sigma_0$ was extracted from the beam spin asymmetry A_{LU} in exclusive $p(e,e'\pi^+)n$ in the KaonLT experiment at Jefferson Lab Hall C. A_{LU} was measured using a 10.6 GeV longitudinally polarized electron beam incident on an unpolarized liquid hydrogen target, with the scattered electron and produced meson detected in two magnetic focusing spectrometers enabling precision cross section measurements. The t-dependence of $\sigma_{LT'}/\sigma_0$ was determined at fixed Q^2 and x_B over a range of kinematics from $2 < Q^2 < 6$ GeV^2 above the resonance region ($W > 2$ GeV). Results are compared to predictions from both the generalized parton distribution (GPD) and Regge formalisms. Furthermore, these data are combined with recent results from CLAS/CLAS12 to determine the Q^2 dependence of $\sigma_{LT'}/\sigma_0$ at fixed x_B and t at two kinematic points.

A quantitative description of simple hadronic systems such as light mesons and nucleons is essential to our understanding of nuclear matter. Deep exclusive meson production (DEMP) reactions, such as $p(e,e'\pi^+)n$, provide opportunities to study the three-dimensional structure of the nucleon through differential cross section and beam- and target-spin asymmetry measurements. The KaonLT experiment (E12-09-011) at Hall C of the Thomas Jefferson National Accelerator Facility (Jefferson Lab or JLab) measured DEMP reactions to extract

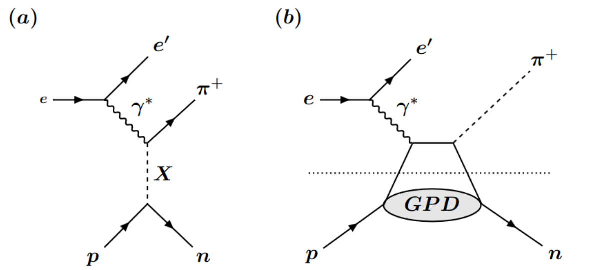

FIG. 1. Exclusive π^+ electroproduction from the proton. (a) A Regge process, in which X represents the exchange of several particles along a Regge trajectory up to a cutoff. (b) Factorization of the reaction into a hard scattering part and a soft part described by a GPD.

a number of hadronic structure observables including σ_L, σ_T, σ_{LT}, σ_{TT}, and $\sigma_{LT'}/\sigma_0$ [1].

DEMP reactions can be conveniently described using three Lorentz invariants. $Q^2 = -(p_e - p_{e'})^2$ is the usual negative of the four-momentum transfer squared of the virtual photon. Additionally, the reaction is characterized by the invariant mass of the virtual photon-nucleon system, $W = \sqrt{m_p^2 + 2m_p(E_e - E_{e'}) - Q^2}$, where m_p is the proton mass, and the Mandelstam variable $t = (p_p - p_n)^2$. Alternately, one may use the Bjorken scaling variable $x_B = Q^2/2m_p(E_e - E_{e'})$ instead of W.

Generalized parton distributions (GPDs) [2, 3] unify the concepts of parton distributions and hadronic form factors by correlating the transverse position and the longitudinal momentum of partons. In the limit of large Q^2 at fixed x_B and t, the $\gamma^* p$ amplitude factorizes into a hard-scattering subprocess and a non-perturbative subprocess described by nucleon GPDs (Fig. 1(b)). The factorization theorem has been proven for longitudinally polarized virtual photons [4, 5], and the contribution of transversely polarized virtual photons can be treated as a twist-3 effect in this approach [6]. GPDs are experimentally accessible through DEMP in the hard-soft factorization regime, but the minimum Q^2 for which factorization may be valid is still unknown [7]. An alternative description of DEMP reactions is based on Regge models. Here, the interaction is mediated by the exchange of meson trajectories in the t channel (Fig. 1(a)). Regge models were first developed for photoproduction (Q^2=0) [8], but have since been extended to DEMP [9]. Their validity does not explicitly rely on hard-soft factorization.

In this work, the cross section ratio $\sigma_{LT'}/\sigma_0$ is extracted from beam-spin asymmetry measurements of $p(e, e'\pi^+)n$. In the one-photon exchange approximation, this asymmetry can be expressed as [10, 11]

$$A_{LU}(Q^2, x_B, t, \phi) = \frac{\sqrt{\epsilon(1-\epsilon)}\frac{\sigma_{LT'}}{\sigma_0}\sin\phi}{1 + \sqrt{2\epsilon(1+\epsilon)}\frac{\sigma_{LT}}{\sigma_0}cos\phi + \epsilon\frac{\sigma_{TT}}{\sigma_0}cos2\phi}, \quad (1)$$

where $\sigma_0 = \sigma_T + \epsilon\sigma_L$ is the unpolarized cross section, ϵ is the ratio of longitudinal and transverse virtual photon polarization, σ_{LT}, σ_{TT}, $\sigma_{LT'}$ are interference cross sections, and ϕ is the azimuthal angle between the electron scattering plane and the hadron reaction plane [12]. All three interference terms are required to vanish when $t = -|t|_{min}$ and $t = -|t|_{max}$, as for these values the $\gamma^* p \to \pi^+ n$ reaction is collinear in the struck proton rest system and ϕ is undefined. The subscript LU specifies the asymmetry resulting from a longitudinally polarized incident electron beam and an unpolarized target, and $\sigma_{LT'}/\sigma_0$ is accessible only in the case of a longitudinally polarized electron beam. $\sigma_{LT'}/\sigma_0$ is extracted from the asymmetry via the $\sin\phi$ moment of A_{LU}, defined as $A_{LU}^{\sin\phi} = \sqrt{2\epsilon(1-\epsilon)}\sigma_{LT'}/\sigma_0$.

This work compares $\sigma_{LT'}/\sigma_0$ to predictions from three models to explore if a GPD or Regge description is more applicable to DEMP reactions at these kinematics. The Goloskokov-Kroll (GK) model [6, 13] calculates $\sigma_{LT'}$ for deep exclusive π^+ production in terms of the twist-2 longitudinal ($\widetilde{E}, \widetilde{H}$) and twist-3 transverse (E_T, H_T) GPDs, with inclusion of the pion pole contributions. For π^+ production, the contribution of the GPD H_T is significant [6], therefore polarized π^+ observables can be used to probe fundamental observables such as the still unknown tensor charge of the nucleon, which is calculated from the integral of H_T [14].

The Vrancx-Ryckebush (VR) model considers Reggeized $\pi(140)$, $\rho(770)$, and $a_1(1260)$ exchange. Including only $\pi(140)$ and $\rho(770)$ leads to a vanishing A_{LU}. The inclusion of the axial-vector $a_1(1260)$ exchange generates a non-zero A_{LU} through interference with the vector $\rho(770)$ exchange [15]. However, this interference is still insufficient to reproduce A_{LU} from previous CLAS data [16] without proper treatment of the "resonant effect" caused by nucleon form factors [15]. The VR model is an extension of the earlier Kaskulov-Mosel model [15], using a different resonant form factor, resulting in better agreement with previous JLab data [17].

The Yu-Choi-Kong (YCK) model also predicts A_{LU} using Regge propagators. This model represents an extension of the Regge model for pion photoproduction [18] to electroproduction. It incorporates the exchange of tensor meson $a_2(1320)$ with axial mesons a_1 and $b_1(1235)$, which were not included in the earlier version [19]. In the new model, the electromagnetic form factors (EMFFs) of the nucleon are considered in two distinct categories: the GPD-mediated form [20], designated YCK1, and the typical dipole form, designated YCK2. In both approaches, the contribution of the magnetic moment term of the nucleon with the Pauli form factor $F_2(Q^2)$ provides a more accurate description of A_{LU}.

A_{LU} is experimentally calculated as a fractional difference of events based on the helicity of the incident electron $N^{\pm}$.

$$A_{LU} = \frac{1}{P}\left(\frac{N^+ - N^-}{N^+ + N^-}\right), \delta_{stat} = \frac{2}{P}\sqrt{\frac{N^+N^-}{(N^+ + N^-)^3}} \quad (2)$$

A_{LU} has been previously measured above the resonance region at Jefferson Lab Hall B in exclusive π^+ production in Refs. [21, 22], and in exclusive π^0 in [23]. This is the first reported measurement of A_{LU} in exclusive $p(e, e'\pi^+)n$ from Hall C as part of the KaonLT experiment [1], with significantly finer kinematic binning and cleaner identification of the exclusive final state.

A continuous wave electron beam with energy 10.585 GeV and beam current up to 70 μA was used. The beam energy was determined to $\pm$3.6 MeV by measuring the bend angle of the beam into Hall C, as it traversed a set of dipole magnets with precisely calibrated field integrals [24]. The beam helicity was flipped at a frequency of 30 Hz in a pseudo-random sequence, with a charge asymmetry of about 0.1% [25]. No dedicated beam polarization measurements were made in Hall C. Rather, Mott polarimetry measurements at the injector to the accelerator ($90 \pm 1\%$) [26], and a calculation of the spin precession through the accelerator indicated that for this beam energy Hall C receives 99% of the source polarization. These gave a result of $89^{+1}_{-3}\%$ longitudinal beam polarization to Hall C, where the uncertainty is determined from the beam energy uncertainty and the range of possible linac energy imbalance.

The electrons were incident upon a 10 cm (762 mg/cm^2) cryogenic unpolarized liquid hydrogen target. Two aluminum foils placed 10 cm apart were used for subtraction of the background from the aluminum end caps of the hydrogen target cell. Beam quality was assured by continuous measurements from three beam position monitors [27], four beam current monitors [28], and an Unser monitor [29].

Charged π^+ were detected in the recently commissioned 11 GeV/c Super High Momentum Spectrometer (SHMS, momentum acceptance $\Delta p/p$ from -10 to +20%, solid angle $\Delta\Omega = 4$ msr [30]), in coincidence with scattered electrons detected in the 7 GeV/c High Momentum Spectrometer (HMS, momentum acceptance $\Delta p/p = \pm 8\%$, solid angle $\Delta\Omega = 7$ msr [31]). Both spectrometers include two drift chambers for track reconstruction, hodoscope arrays for triggering, Čerenkov detectors and lead-glass calorimeters for particle identification. Positively charged pions were identified in the SHMS using an aerogel Čerenkov detector with refractive index $n = 1.015$ (for $p_\pi < 5$ GeV/c) or $n = 1.011$ (for $p_\pi > 5$ GeV/c). Electrons were identified in the HMS via a gas Čerenkov detector filled with C_4F_{10} with refractive index 1.0008 in combination with the lead-glass

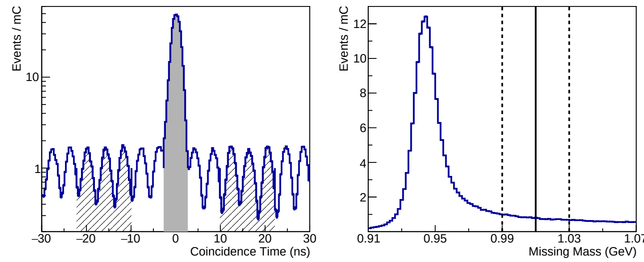

FIG. 2. Coincidence time and missing mass spectra for Q^2=3.0 GeV^2, x_B=0.25, center SHMS setting. Left: coincidence time between the HMS and SHMS. The prompt peak selected is highlighted in grey, and the windows used to subtract random coincidences are filled in with lines. Right: the missing mass distribution of $p(e, e'\pi^+)n$. The solid line shows the missing mass cut used, and the dashed lines show the variation of the cut used to calculate a cut dependence as a systematic error.

calorimeter. Any remaining contamination from real $e-p$ and $e - K^+$ coincidences were eliminated with a coincidence time cut of $\pm$2.25 ns. Background from aluminum target cell walls (1–2% of the yield) and random coincidences ($\sim$3% of the yield at x_B=0.4 and $\sim$12% at x_B=0.25) were subtracted from charge normalized yields. The exclusive neutron final state was selected with a cut of m_m <1.01 GeV on the reconstructed missing mass $m_m^2 = (p_e - p_{e'} - p_\pi)^2$, which in the case of the $p(e, e'\pi^+)n$ reaction should be close to the free neutron mass (Fig. 2). As the detector inefficiencies and data acquisition livetimes are uncorrelated with the electron beam helicity, they cancel in the calculation of A_{LU} (Eqn. 2).

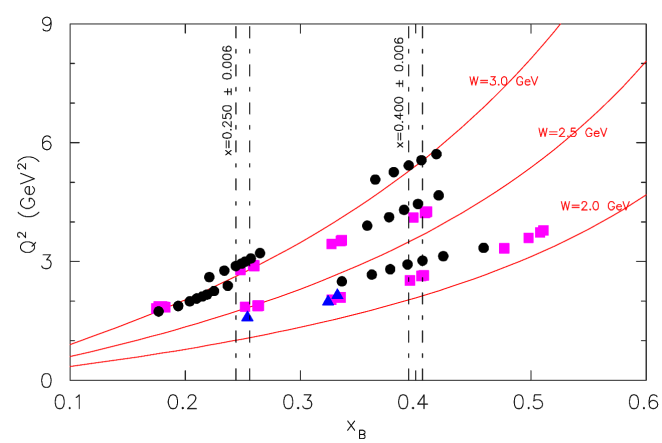

FIG. 3. Phase space plot of the kinematics for which $\sigma_{LT'}/\sigma_0$ has been measured. Legend: Black circles: KaonLT [This work]; Blue triangles: CLAS [21]; Magenta squares: CLAS12 [22]. Only data with $-t < 0.7$ GeV^2 are shown. By combining these data sets, the Q^2 dependence of $\sigma_{LT'}/\sigma_0$ can be determined at fixed x_B and $-t$ at two values of x_B, shown as dashed lines.

The $Q^2 - x_B$ settings studied in this experiment are

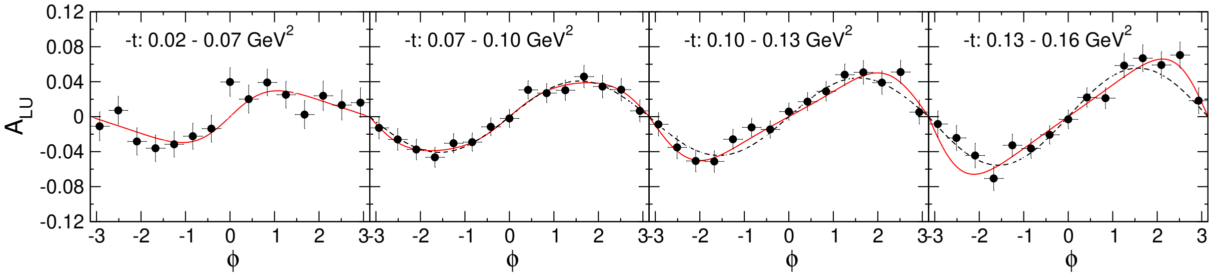

FIG. 4. A_{LU} as a function of ϕ for the first four t-bins for central values of $Q^2 = 3$ GeV^2, x_B =0.25. The solid line shows the full fit and the dashed line the approximated fit. Uncertainties are statistical only.

shown in Fig. 3. This work targets the range $2 < Q^2 < 6$ GeV^2, above the resonance region, $W > 2$ GeV. For each $Q^2 - x_B$ setting, the HMS angle and momentum, as well as the SHMS momentum, were kept fixed. To attain full coverage in ϕ, data were taken with the SHMS at $\pm 3°$ of the $\vec{q}$-vector direction (direction of virtual photon momentum), in addition to the data centered on the $\vec{q}$-vector.

The relevant electroproduction kinematic variables, Q^2, x_B, W, and t were reconstructed from the measured spectrometer quantities. Using the over-determined $p(e, e'p)$ reaction, the beam momentum and the spectrometer central momenta were determined absolutely to $< 0.5\%$, while the incident beam angle and spectrometer central angles were absolutely determined to < 0.5 mrad.

For each $Q^2 - x_B$ setting, the data were split into 5-8 bins in t and 15 bins in ϕ, with the number of bins determined by the raw number of events at each setting. The asymmetry was calculated according to Eqn. 2 for each t-bin. The asymmetry was calculated separately for each of the three SHMS angles, and an error-weighted average taken to obtain a complete ϕ distribution. In exclusive pion production, the experimental acceptances in x_B, Q^2 and t are correlated. Thus, for each t-bin (but independent of ϕ), the mean Q^2 and x_B values of the data vary slightly from the 'central' values. The exact kinematics for each data point are given in the supplemental material [32]. Fig. 4 shows the binned asymmetry for central kinematics of Q^2=3 GeV^2, x_B=0.25.

Previous work assumed that $\sigma_{TT}/\sigma_0 \ll 1$ and $\sigma_{LT}/\sigma_0 \ll 1$, such that Eqn. 1 simplifies to $A_{LU} = A_{LU}^{\sin\phi} \sin\phi$, the justification being that the full functional form and the approximated form gave extremely similar results for $A_{LU}^{\sin\phi}$ [21, 22]. In this work, it was found that the choice of fitting function makes a significant difference in the extracted $A_{LU}^{\sin\phi}$, as seen in the last panel of Fig. 4. The authors are aware of no theoretical constraints for why σ_{LT}/σ_0 and σ_{TT}/σ_0 should be negligible. Therefore, $A_{LU}^{\sin\phi}$ was determined using the full functional form of Eqn. 1, and the difference between this result and that obtained using the approximated fit was used as a systematic uncertainty. Since such a difference is unidirectional, the total systematic error (obtained from the quadrature sum of systematic uncertainties) is asymmetric, denoted $\delta^{\uparrow}_{sys}$ and $\delta^{\downarrow}_{sys}$ for the upper and lower error bars. The other main sources of systematic error were the uncertainty on the beam polarization and the dependence of $A_{LU}^{\sin\phi}$ on the exact values used for the coincidence time and missing mass cuts. The statistical error on $A_{LU}^{\sin\phi}$ is taken as the error of fitting when including the statistical uncertainties per ϕ bin.

The cross section ratio $\sigma_{LT'}/\sigma_0$ and its uncertainty were then extracted from $A_{LU}^{\sin\phi}$. The polarization contributed an uncertainty of 3.4%, and the cut dependence contributed between 1–7%, with one outlier at 12%. The point-to-point uncertainty was dominated by the method of fit, which contributed an average error of 12%, but for one t-bin contributed 70%. Exact values of $\sigma_{LT'}/\sigma_0$ and its uncertainties are available in [32].

Fig. 5 shows $\sigma_{LT'}/\sigma_0$ compared to predictions from five theoretical models. The VR model agrees with the data reasonably well at low $-t$, but does not capture the plateau of $\sigma_{LT'}/\sigma_0$ that occurs at higher $-t$. GK1 shows significantly better agreement for $x_B = 0.40$ than for $x_B = 0.25$, in which case the t dependence does not match the prediction. In Ref. [22], the argument was made that increasing the GPD H_T in the GK calculation resulted in good agreement with experimental data. In this work, the curve GK2 has a lower magnitude, bringing it closer to data than GK1, but it still does not re-create the shape properly at all kinematics. The best agreement with this work is the YCK model. YCK2 underestimates $\sigma_{LT'}/\sigma_0$, but YCK1 provides a reasonable prediction of both the magnitude and t-dependence of $\sigma_{LT'}/\sigma_0$. Since this data is in the QCD transition regime, it is not unexpected that a combined Regge and GPD prediction would give the best description of experimental results.

These results are in good agreement with recent results from CLAS12, showing a similar magnitude and t dependence of $\sigma_{LT'}/\sigma_0$ [22]. At points with very similar Q^2, x_B and t, the KaonLT and CLAS12 measurements agree within the quoted uncertainties. Furthermore, by comparing data between CLAS, CLAS12, and this work, two kinematics were identified to determine the Q^2 de-

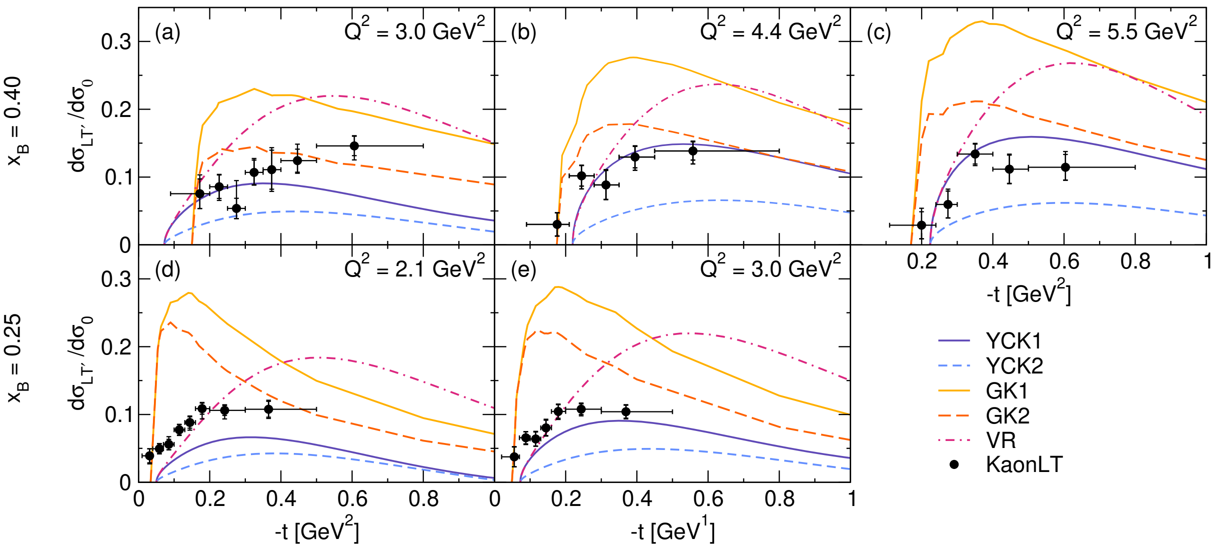

FIG. 5. The extracted $\sigma_{LT'}/\sigma_0$ as a function of t for each $Q^2 - x_B$ setting. The horizontal error bar indicates the width of the t-bin, and the double vertical error bar shows the statistical and total errors. The smooth curves represent theory predictions, evaluated at the central kinematics of each $Q^2 - x_B$ setting. GK1 refers to the default GK version [33], and GK2 is the GK model with the modification of $H_T \to H_T * 2$, following the example of Ref. [22]. YCK1 is the YCK model with the nucleon EMFFs parametrized with GPDs, whereas YCK2 uses a dipole parametrization.

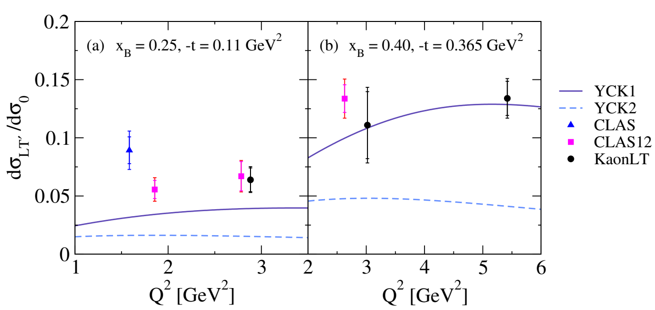

FIG. 6. Values of $\sigma_{LT'}/\sigma_0$ from three different experiments [21, 22] [This work] plotted as a function of Q^2 at fixed x_B and $-t$. The Q^2 dependence is consistent, within error, with a horizontal line.

pendence of $\sigma_{LT'}/\sigma_0$, the first at $x_B = 0.250 \pm 0.006$, $t = 0.110 \pm 0.006$, and the second at $x_B = 0.400 \pm 0.006$, $t = 0.365 \pm 0.015$. At the two $x_B - t$ values investigated, the asymmetry was largely independent of Q^2 (Fig. 6). In Fig. 5, it can be seen that all theory curves incorporate a Q^2 dependence, in which the magnitude of the predicted $\sigma_{LT'}/\sigma_0$ increases with Q^2. This work suggests that in this regime, a description involving a Q^2 dependence is not entirely accurate.

In summary, the observable A_{LU} and the structure function ratio $\sigma_{LT'}/\sigma_0$ of the $p(e, e'\pi^+)n$ reaction have been measured at Hall C of Jefferson Lab over a wide range of kinematics. The dependence of $\sigma_{LT'}/\sigma_0$ on t at fixed Q^2 and x_B has been explored and compared to theoretical calculations. The best agreement is with YCK1, a Regge-based model in which the nucleon EMFFs are parametrized with GPDs. Based on this, and the fact that both the VR and GK models predicted some characteristics of the data, a combined Regge and GPD description is thought to be most applicable to these results. Additionally, the dependence on Q^2 at fixed x_B and t was found to be flat, a feature which was predicted by none of the theoretical calculations. Future work with KaonLT data will include measurements of $\sigma_{LT'}/\sigma_0$ in $p(e, e'\pi^+)\Delta^0$ and u-channel meson production.

We thank the staff of the Accelerator and the Physics Divisions at Jefferson Lab for the excellent efforts during the experimental data taking. This work is supported by the Natural Sciences and Engineering Research Council of Canada (NSERC) SAPIN-2021-00026 and a Canadian Institute of Nuclear Physics Graduate Fellowship. Additional support from the University of Regina is gratefully acknowledged.

This material is based upon work supported by the U.S. Department of Energy, Office of Science, Office of Nuclear Physics under contract DE-AC05-06OR23177. Support is also acknowledged from NSF grants PHY 2309976, 2012430 and 1714133 at the Catholic University of America, UK Science and Technology Facilities Council (STFC) grants ST/V001035/1 and ST/W004852/1 at the University of York, and NSF grant PHY 2209199 at Ohio University.

[1] T. Horn, G. M. Huber, P. Markowitz, *et al.*, Studies of the L/T Separated Kaon Electroproduction Cross Sections

from 5-11 GeV (2008), Jefferson Lab 12 GeV Experiment E12-09-011.

[2] D. Müller, Generalized parton distributions: Visions, basics, and realities, Few-Body Syst. **55**, 317 (2014).

[3] M. Diehl, Generalized parton distributions, Phys. Rep. **388**, 41 (2003).

[4] A. V. Radyushkin, Asymmetric gluon distributions and hard diffractive electroproduction, Phys. Lett. B **385**, 333 (1996), arXiv:hep-ph/9605431.

[5] J. C. Collins, L. Frankfurt, and M. Strikman, Factorization for hard exclusive electroproduction of mesons in QCD, Phys. Rev. D **56**, 2982 (1997).

[6] S. V. Goloskokov and P. Kroll, An attempt to understand exclusive π^+ electroproduction, Eur. Phys. J. C **65**, 10.1140/epjc/s10052-009-1178-9 (2009).

[7] Favart, L., Guidal, M., Horn, T., and Kroll, P., Deeply virtual meson production on the nucleon, Eur. Phys. J. A **52**, 158 (2016).

[8] M. Guidal, J.-M. Laget, and M. Vanderhaeghen, Pseudoscalar meson photoproduction at high energies: from the Regge regime to the hard scattering regime, Phys. Lett. B **400**, 6 (1997).

[9] M. Vanderhaeghen, M. Guidal, and J.-M. Laget, Regge description of charged pseudoscalar meson electroproduction above the resonance region, Phys. Rev. C **57**, 1454 (1998).

[10] M. Diehl and S. Sapeta, On the analysis of lepton scattering on longitudinally or transversely polarized protons, Eur. Phys. J. C **41**, 515–533 (2005).

[11] T. Arens, O. Nachtmann, M. Diehl, and P. V. Landshoff, Some tests for the helicity structure of the pomeron in e p collisions, Z. Phys. C **74**, 651 (1997), arXiv:hep-ph/9605376.

[12] A. Bacchetta, U. D'Alesio, M. Diehl, and A. Miller, Single-spin asymmetries: The trento conventions, Physical Review D: Particles and fields **70** (2004).

[13] S. V. Goloskokov and P. Kroll, Transversity in hard exclusive electroproduction of pseudoscalar mesons, Eur. Phys. J. A **47**, 112 (2011), arXiv:1106.4897 [hep-ph].

[14] G. R. Goldstein, J. O. G. Hernandez, and S. Liuti, Flexible parametrization of generalized parton distributions: The chiral-odd sector, Phys. Rev. D **91**, 114013 (2015).

[15] M. M. Kaskulov and U. Mosel, Deep exclusive charged π electroproduction above the resonance region, Phys. Rev. C **81**, 045202 (2010).

[16] M. G. Alekseev, V. F., *et al.*, Azimuthal asymmetries of charged hadrons produced by high-energy muons scattered off longitudinally polarised deuterons, The European Physical Journal C **70**, 39–49 (2010).

[17] T. Vrancx and J. Ryckebusch, Charged pion electroproduction above the resonance region, Phys. Rev. C **89**, 025203 (2014), arXiv:1310.7715 [nucl-th].

[18] B. G. Yu, T. K. Choi, and W. Kim, Regge phenomenology of pion photoproduction off the nucleon at forward angles, Phys. Rev. C **83**, 025208 (2011).

[19] T. K. Choi, K. J. Kong, and B. G. Yu, Pion and proton form factors in the regge description of electroproduction $p(e, e'\pi^+)n$, J. Korean Phys. Soc. **67**, 1089–1094 (2015).

[20] M. Guidal, M. V. Polyakov, A. V. Radyushkin, and M. Vanderhaeghen, Nucleon form factors from generalized parton distributions, Phys. Rev. D **72**, 054013 (2005).

[21] S. Diehl *et al.* (The CLAS Collaboration), Extraction of beam-spin asymmetries from the hard exclusive π^+ channel off protons in a wide range of kinematics, Phys. Rev. Lett. **125**, 182001 (2020).

[22] S. Diehl *et al.*, A multidimensional study of the structure function ratio $\sigma_{LT'}/\sigma_0$ from hard exclusive π^+ electroproduction off protons in the GPD regime, Phys. Lett. B **839**, 137761 (2023).

[23] R. De Masi *et al.* (CLAS Collaboration), Measurement of $ep \to ep\pi^0$ beam spin asymmetries above the resonance region, Phys. Rev. C **77**, 042201 (2008).

[24] D. W. Higinbotham, Using Polarimetry To Determine The CEBAF Beam Energy, PoS Proc. Sci. **PSTP2013**, 014 (2013).

[25] J. Benesch, A. Bogacz, A. Freyberger, Y. Roblin, T. Satogata, R. Suleiman, and M. Tiefenback, *12 GeV CEBAF Beam Parameter Tables*, Tech. Rep. (Jefferson Laboratory, 2018) jLAB-TN-18-022.

[26] J. M. Grames, C. K. Sinclair, M. Poelker, X. Roca-Maza, M. L. Stutzman, R. Suleiman, M. A. Mamun, M. McHugh, D. Moser, J. Hansknecht, B. Moffit, and T. J. Gay, High precision 5 MeV Mott polarimeter, Phys. Rev. C **102**, 015501 (2020).

[27] J. Benesch *et al.*, Jefferson Lab Hall C: Precision Physics at the Luminosity Frontier, arXiv:2209.11838 [nucl-ex] (2022).

[28] D. J. Mack, Beam current monitors for Hall C, AIP Conf. Proc. **269**, 527 (1992), https://pubs.aip.org/aip/acp/article-pdf/269/1/527/11825722/527_1_online.pdf.

[29] K. B. Unser, The parametric current transformer, a beam current monitor developed for LEP, AIP Conf. Proc. **252**, 266 (1992), https://pubs.aip.org/aip/acp/article-pdf/252/1/266/11666911/266_1_online.pdf.

[30] S. Ali *et al.*, The SHMS 11 GeV/c Spectrometer in Hall C at Jefferson Lab, To be published.

[31] H. P. Blok *et al.* (Jefferson Lab F_π Collaboration), Charged pion form factor between $Q^2 = 0.60$ and 2.45 GeV^2. I. Measurements of the cross section for the ^{1}H$(e, e'\pi^+)n$ reaction, Phys. Rev. C **78**, 045202 (2008).

[32] See Supplemental Material for tabulated values of the kinematics and $\sigma_{LT'}$ for all data points.

[33] B. Berthou, D. Binosi, N. Chouika, M. Guidal, C. Mezrag, H. Moutarde, F. Sabatié, P. Sznajder, and J. Wagner, PARTONS: PARtonic Tomography Of Nucleon Software. A computing platform for the phenomenology of Generalized Parton Distributions, Eur. Phys. J. C **78** (2015).